RESEARCH PAPER | Engineering | Volume : 4 | Issue : 9 | September 2014 | ISSN - 2249-555X

Comparative Analysis of Emissions Using CFD for Two Types of Combustion Chamber Geometryin A Diesel Engine

KEYWORDS: ANSYS FLUENT, CFD, Combustion Chamber Geometry, Diesel Engine.

Lokesh Aurangabadkar
PG scholar, Department of Mechanical Engineering, Institute of Engineering and Technology, Devi Ahilya Vishwavidyalaya, Indore, MP, INDIA.

Ibrahim Hussain Shah
Assistant Professor, Department of Mechanical Engineering, Institute of Engineering and Technology,Devi Ahilya Vishwavidyalaya, Indore, MP, INDIA.

ABSTRACT *The objective of the present investigation is to assess the influence of the combustion chambers geometry on temperature distribution and engine emissions. A computational fluid dynamics (CFD) Code ANSYS FLUENT has been used for modelling the combustion chamber geometry and for its analysis. In particular two different combustion chamber geometries were investigated. To perform this work, a 30o sector of Diesel Engine Combustion chamber is modelled for two different geometries. In first case a 30o sector of Toroidal Combustion Chamber is modelled using ANSYS 14.0. This geometry under observation was analysed, by giving various operating parametric inputs and results were obtained for emission of NO, N2O, CO, CO2 along with the temperature profile. In second case the 30o sector of a Re-Entrant combustion chamber is modelled and same process has been adopted for this geometry. In the end the results for the two geometries are compared.*

INTRODUCTION

Engine manufacturers, facing more and more Complex emission standards concerning environmental regulations, are producing their efforts to reduce Engine emissions. One of the feasible emission control strategies consists in reducing the engine pollutant concentration by modifying the combustion chamber geometry. The development of a procedure able to control the Engine emissions requires the knowledge of where NO_x and other pollutants are formed as well as their mechanisms of formation. Many studies have been carried out to clarify the effect of combustion chamber geometry on engine emission formation. The combustion chamber geometry is basically carried by the piston top.

One of the biggest advancements in Engine technology is the use of different piston "tops" or "crowns," the part that enters the combustion chamber and is subjected to combustion. While older piston tops were mostly flat, many of the new features bowls on top that have different effects on the combustion process. Diesels don't have an ignition phase, so the piston crown itself may form the combustion chamber. These engines often use pistons with differently shaped crowns, although with direct injection becoming increasingly popular, gasoline engines are starting to use them as well. The combustion chamber geometry of the Diesel engine also effects the engine emissions. This study looks up on the effect of Toroidal and Re-entrant combustion chamber geometry on the exhaust emission at an engine speed 2000 rpm.

METHODOLOGY

The methodology adopted for the present work is as follows:

- Solid modelling of the Toroidal combustion chamber geometry with fuel injector.
- Mesh generation. Solution of the governing equations with appropriate boundary conditions.
- Solid modelling of the Re-entrant combustion chamber geometry with fuel injector.
- Mesh generation. Solution of the governing equations with appropriate boundary conditions.
- Comparison of the simulated results for the two combustion chamber geometries.

The study is expected to explore the potential of using CFD tool for design and optimisation of combustion chamber geometry. The commercial CFD code ANSYS FLUENT 14.0 is used for the analysis of flow. The CFD package includes user interfaces to input problem parameters and to examine the results. The code contains three elements

1. Pre-Processor
2. Solver
3. Post Processor

Pre-processor mainly involves the creation of basic 3D model, grid generation and fixing of the boundary conditions. Layering approach is adopted in FLUENT. For the approach mentioned above, in-cylinder problems solved in Fluent consist of three stages. The first stage is to decompose the geometry into different zones and mesh them properly. By breaking up the model into different zones, it is possible to apply different mesh motion strategies to different regions in a single simulation. The second stage is to setup the Geometry inside the Fluent with the help of a setup journal. The third stage is to perform a transient in-cylinder simulation.

CFD ANALYSIS

There are mainly three equations we solve in computational fluid dynamics problem. They are Continuity equation,Momentum equation (Navier Stokes equation) and Energy equation. The flow of most fluids may be analysed mathematically by the use of two equations. The first, often referred to as the Continuity Equation, requires that the mass of fluid entering a fixed control volume either leaves that volume or accumulates within it. It is thus a "mass balance" requirement imposed in mathematical form, and is a scalar equation. The other governing equation is the Momentum Equation, or Navier-Stokes Equation, and may be thought of as a "momentum balance". The Navier-Stokes equations are vector equations, mean-

Volume : 4 | Issue : 9 | September 2014 | ISSN - 2249-555X

ing that there is a separate equation for each of the coordinate directions (usually three).

MATHEMATICAL MODEL

In this thesis RNG k- ε model were employed because, in this model 'k' is the turbulence kinetic energy and is defined as the variance of the fluctuations in velocity. It has dimensions of (L^2 T^{-2}), e.g. m^2/s^2. 'ε' is the turbulence eddy dissipation (the rate at which the velocity fluctuations dissipate) and has dimensions of k per unit time (L^2 T^{-3}), e.g. m^2/s^3.

$$\frac{\partial k}{\partial t} + u_j \frac{\partial k}{\partial x_j} = \tau_{ij} \frac{\partial u_i}{\partial x_j} - \varepsilon + \frac{\partial}{\partial x_j}\left[\nu + \upsilon_t / \sigma_k \frac{\partial k}{\partial x_j}\right]$$

$$\tau_{ij} = -\overline{u_i u_j} = 2\upsilon_t S_{ij} - \frac{2}{3} k \delta_{ij}$$

The turbulent kinetic energy equation as modelled has a number of simplifications from the rigorous equation.

The first term on the RHS is the production of 'k', the second term 'ε'is the specific dissipation per unit mass. The last term describe the transport of 'k' by molecular and turbulent diffusion.

$$\frac{\partial k}{\partial t} + u_j \frac{\partial k}{\partial x_j} = \tau_{ij} \frac{\partial u_i}{\partial x_j} - \varepsilon + \frac{\partial}{\partial x_j}\left[\nu + \upsilon_t / \sigma_k \frac{\partial k}{\partial x_j}\right]$$

$$\frac{\partial \varepsilon}{\partial t} + u_j \frac{\partial \varepsilon}{\partial x_j} = C_{\varepsilon 1} \frac{\varepsilon}{k} \tau_{ij} \frac{\partial u_i}{\partial x_j} - C_{\varepsilon 2} \frac{\varepsilon^2}{k} + \frac{\partial}{\partial x_j}\left[\nu + \upsilon_t / \sigma_\varepsilon \frac{\partial \varepsilon}{\partial x_j}\right]$$

$$\upsilon_t = C_\mu k^2 / \varepsilon$$

This model was derived and tuned for Flows with high Reynolds numbers. This implies that it is suited for flows where the turbulence is nearly iso-tropic and is suited to flows where the energy cascade proceeds in local equilibrium with respect to generation.

PROBLEM FORMULATION

Both the Combustion Chamber geometries are obtained by trimming the piston head. Piston Head is the upper part of the Piston which is exposed to combustion. Here, due to the limitations in computing resources, 30 degree of the3-D sector geometry is only selected for study. Table 1 Shows the engine in-cylinder data and fuel injection details. The computations are carried out by FLUENT solver. The time accurate computations are performed on a Intel Core i7 processor (3.50 GHz, 16 GB RAM).

Table 1: Engine data and fuel injection details [1]

Engine	4 – S Diesel Engine
Bore	130 mm
Stroke	150 mm
R.P.M.	2000
Length Of Connecting Rod	275 mm
Compression Ratio	15.5
Fuel	Diesel
Fuel Injection Quantity	207 mg/Cycle
Injection Hole Diameter	148 X 10^{-6} m
Injected Mass	0.0144 g
Equivalence Ratio	0.67
Swirl Ratio	2

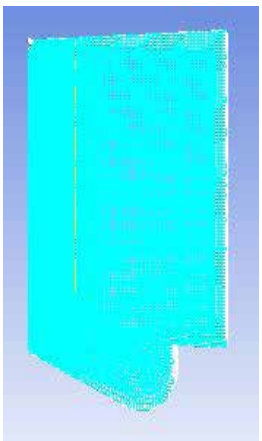

Figure 1(a) : Mesh view of Toroidal Geometry

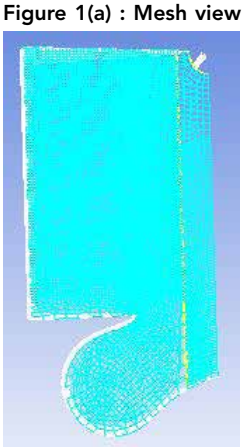

Figure 1(b) : Mesh view of Re-entrant Geometry

Total no. of nodes in Toroidal Geometry is 131379 and no. of elements are 116756. In Re-Entrant Geometry no. of nodes are 96303 and no. of elements are 86928.

CFD RESULTS (TEMPERATURE PROFILES)

The following contours show the Temperature Profile for wo different Combustion Chamber geometry. The range is given on the coloured scale. The Temperature at any point of contour can be obtained by matching the colour of contour at desired point with the colour on the scale and its corresponding numeric value will be obtained.

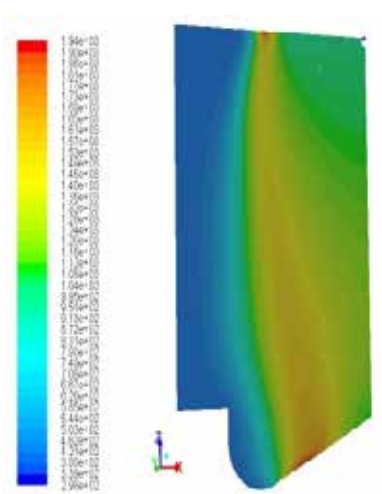

Figure 2(a) : Temperature Profile of Toroidal Geometry

Volume : 4 | Issue : 9 | September 2014 | ISSN - 2249-555X

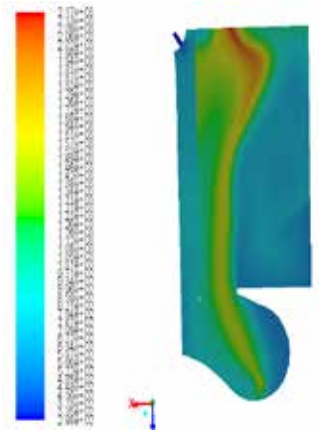

Figure 2(a) : Temperature Profile of Toroidal Geometry

RESULTS AND DISCUSSION

MASS FRACTION OF NO vs TEMPERATURE

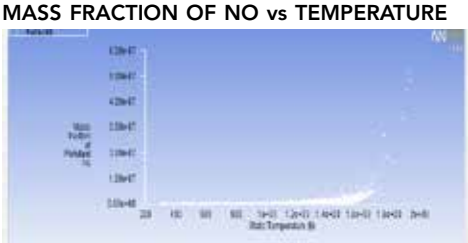

Figure 3(a) :Mass fraction of NO vs Temperature plot for Toroidal Geometry

The Graph is plotted between mass fraction of NO (0 to 6 X 10 $^{-7}$) vs Temperature (200K to 2000K) and maximum value of mass fraction of NO is obtained around 2000K which is around 5.2 X 10 $^{-7}$.

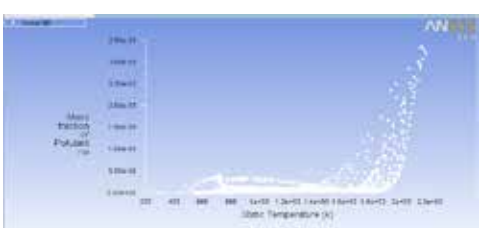

Figure 3(b) : Mass fraction of NO vs Temperature plot for Re-entrant Geometry

The Graph is plotted between mass fraction of NO (0 to3.5 X 10 $^{-5}$) vs Temperature (200K to 2200K) and maximumvalue of mass fraction of NO is obtained around 2100K which is around 3.5 X 10 $^{-5}$.

MASS FRACTION OF N_2O vs TEMPERATURE

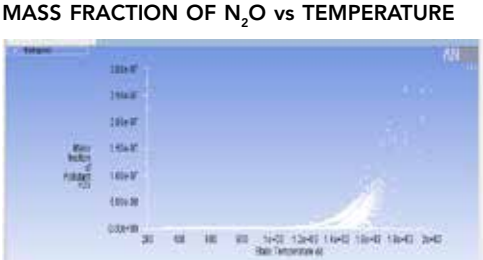

Figure 4(a) : Mass fraction of N_2O vs Temperature plot for Toroidal Geometry

The Graph is plotted between mass fraction of N_2O (0 to 3 X 10 $^{-7}$) vs Temperature (200K to 2000K) and maximum value of mass fraction of N_2O is obtained around 1900K which is around 3 X 10 $^{-7}$.

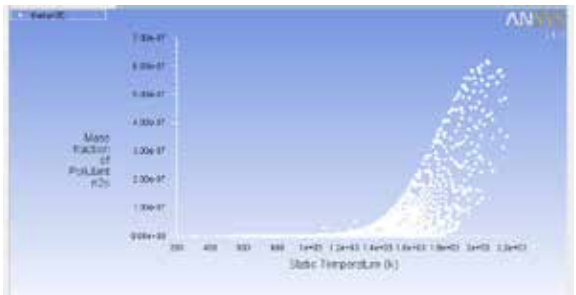

Figure 4(b) : Mass fraction of N_2O vs Temperature plot for Re-entrant Geometry

The Graph is plotted between mass fraction of N_2O(0 to7 X 10 $^{-7}$) vs Temperature (200K to 2200K) and maximum value of mass fraction of N_2O is obtained around 2000K which is around 6.5 X 10 $^{-7}$.

MASS FRACTION OF CO vs TEMPERATURE

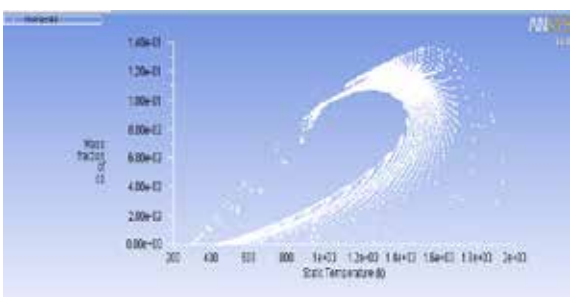

Figure 5(a) : Mass fraction of CO vs Temperature plot for Toroidal Geometry

The Graph is plotted between mass fraction of CO (0 to 0.14) vs Temperature (200K to 2000K) and maximum value of mass fraction of CO is obtained around 1600K which is around 0.14.

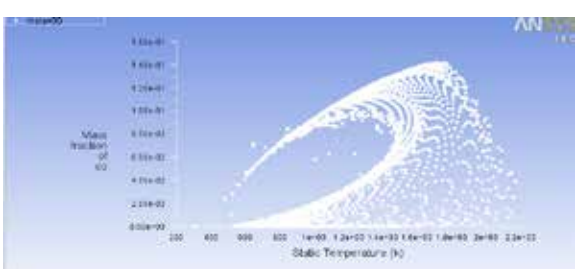

Figure 5(b) : Mass fraction of CO vs Temperature plot for Re-entrant Geometry

The Graph is plotted between mass fraction of CO (0 to 0.16) vs Temperature (200K to 2000K) and maximum value of mass fraction of CO is obtained around 1800K which is around 0.15.

MASS FRACTION OF CO_2 vs TEMPERATURE

Volume : 4 | Issue : 9 | September 2014 | ISSN - 2249-555X

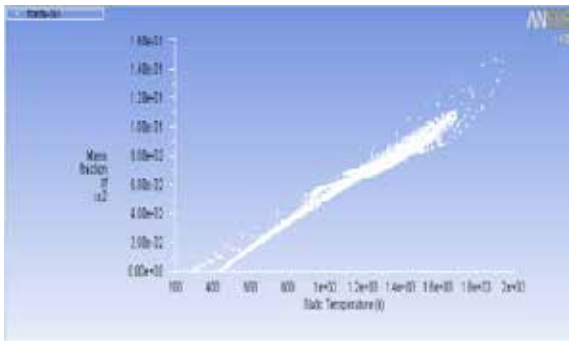

Figure 6(a) : Mass fraction of CO_2 vs Temperature plot for Toroidal geometry

The Graph is plotted between mass fraction of CO_2 (0 to 0.16) vs Temperature (200K to 2000K) and maximum value of mass fraction of CO_2 is obtained around 1800K which is around 0.15.

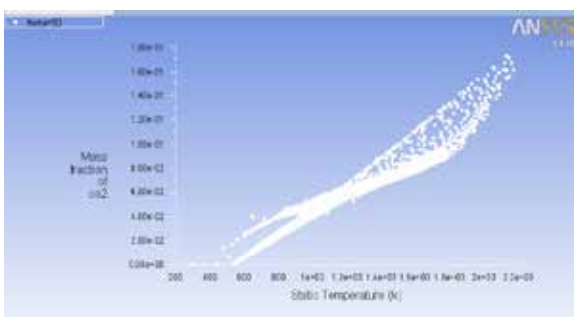

Figure 6(b) : Mass fraction of CO_2 vs Temperature plot for Re-entrant Geometry

The Graph is plotted between mass fraction (0 to 0.18) of CO_2 vs Temperature (200K to 2000K) and maximum value of mass fraction of CO_2 is obtained around 2100K which is around 0.18.

CONCLUSION

The CFD results for engine emissions from both cases of combustion chambers were obtained at engine speeds of 2000 rpm. On comparing these results we have observed that, the maximum value of mass fraction of NO is higher in Re-entrant geometry. We have also observed that the maximum value of mass fraction of N_2O is higher in Re-entrant geometry but there is a very small difference between the two values. The maximum temperature achieved is also higher in case of Re-entrant geometry.similarly the maximum values in case of oxides of carbon are also on the higher side for the Re-entrant geometry.

The main cause of the variation of emission results between the two combustion chambers is difference in geometry for them. Because the geometry of the combustion chamber affects the flow pattern, fuel injection, swirl generated inside the chamber, squish behavior.

Thus on the basis of above observations, it can be concluded that for same input conditions for engine operations and fuel injection values, Toroidal geometry will produce less pollutants as well as the temperature achieved within the Toroidal combustion chamber will be comparatively lesser.

ACKNOWLEDGEMENT

We are thankful to Medi-Caps Institute of Technology and Management, Indore, M.P. India for providing technical assistance in CFD work with ANSYS FLUENT.

REFERENCE

[1] R. Manimaran & R.T.K. Raj, "Effect of Swirl in a Constant Speed DI Diesel Engine using Computational Fluid Dynamics", CFD Letters, Vol. 4 (4) – December 2012. | [2] G. Sucharitha, & A. Kumarswamy, "Analysis on Three – Dimensional Flow of DI Diesel Engine for different Piston Configurations using CFD", Indian Journal Of Science And Technology, Supplementary Article, P. 4748-4753. Vol. 6 – May 2013. | [3] De Risi, D. F. Manieri & D. Laforgia, "A Theoritical Investigation on the Effects of Combustion Chamber Geometry and Engine Speed on Soot and NOX Emissions", ASME, ICE, Camere. | [4] Raouf Mobasheri & Zhijun Peng,"CFD Investigation of the Effects of Re-Entrant Combustion Chamber Geometry in a HSDI Diesel Engine". World Academy of Science, Engineering and Technology, International Journal of Mechanical, Industrial Science and Engineering Vol.7 No.4, 2013 | [5] Arturo De Risi, Teresa Donateo & Dominico Leforgia, "Optimization of Combustion Chamber of DI Diesel Engine". SAE, 2003-01-1064. | [6] Sushma H., "CFD Modelling of the In-Cylinder Flow in DI Diesel Engine". International Journal of Scientific and Research Publications, Volume 3, Issue 12, December 2013. | [7] Rajshekhar C.R., Chandrashekhar T.K., Umashankar Chebbiyan.,and Rajgopal H.K,"Studies on Effects of Combustion Chamber Geometry and Injection Pressure on Biodiesel Combustion".Canadian Society of Mechanical Engineering, Vol. 36, No. 4, 2012 | [8] Mamilla V.R., Mallikarjuna M.V. & Dr.G.L.N. Rao "Effect of Combustion Chamber Design on a DI Diesel Engine Fuelled with Jatropha Methyle Esters Blends with Diesel." International Conference on Design and Manufacturing, ICDM 2013. Procedia Engineering 64 (2013) 479 – 490. | [9] Sung Wook Park, "Optimization of Combustion Chamber Geometry for Stoichiometric Diesel Combustion using a micro Genetic Algorithm", Fuel Processing Technology 91 (2010) 1742 – 1752. |